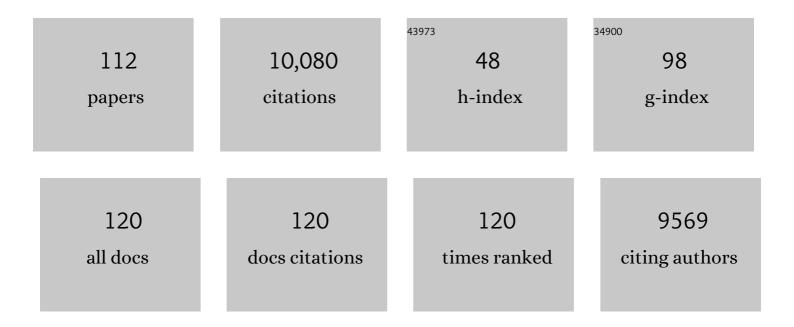
List of Publications by Year in descending order

Source: https://exaly.com/author-pdf/8794636/publications.pdf Version: 2024-02-01



FLENA OPLOVA

#	Article	IF	CITATIONS
1	A New Generation of the IMAGIC Image Processing System. Journal of Structural Biology, 1996, 116, 17-24.	1.3	1,182
2	Single-particle electron cryo-microscopy: towards atomic resolution. Quarterly Reviews of Biophysics, 2000, 33, 307-369.	2.4	535
3	Cryo-electron microscopy structure of an SH3 amyloid fibril and model of the molecular packing. EMBO Journal, 1999, 18, 815-821.	3.5	487
4	Atomic structure and hierarchical assembly of a cross-Î ² amyloid fibril. Proceedings of the National Academy of Sciences of the United States of America, 2013, 110, 5468-5473.	3.3	479
5	Structure of the AAA ATPase p97. Molecular Cell, 2000, 6, 1473-1484.	4.5	394
6	Structural Basis of Pore Formation by the Bacterial Toxin Pneumolysin. Cell, 2005, 121, 247-256.	13.5	369
7	The structural basis for membrane binding and pore formation by lymphocyte perforin. Nature, 2010, 468, 447-451.	13.7	364
8	Structure of a type IV secretion system. Nature, 2014, 508, 550-553.	13.7	280
9	Structure of a Type IV Secretion System Core Complex. Science, 2009, 323, 266-268.	6.0	277
10	Arrangement of tRNAs in Pre- and Posttranslocational Ribosomes Revealed by Electron Cryomicroscopy. Cell, 1997, 88, 19-28.	13.5	247
11	The 70S Escherichia coli ribosome at 23 å resolution: fitting the ribosomal RNA. Structure, 1995, 3, 815-821.	1.6	237
12	Structural framework for DNA translocation via the viral portal protein. EMBO Journal, 2007, 26, 1984-1994.	3.5	207
13	Structure of keyhole limpet hemocyanin type 1 (KLH1) at 15 Ã resolution by electron cryomicroscopy and angular reconstitution †1 â€This article is dedicated to the memory of Anneke van Heel. 1Edited by M.F. Moody. Journal of Molecular Biology, 1997, 271, 417-437.	2.0	202
14	Structure of the Escherichia coli ribosomal termination complex with release factor 2. Nature, 2003, 421, 90-94.	13.7	191
15	Electron cryomicroscopy and angular reconstitution used to visualize the skeletal muscle calcium release channel. Nature Structural Biology, 1995, 2, 18-24.	9.7	185
16	3D map of the plant photosystem II supercomplex obtained by cryoelectron microscopy and single particle analysis. Nature Structural Biology, 2000, 7, 44-47.	9.7	172
17	Direct three-dimensional visualization of membrane disruption by amyloid fibrils. Proceedings of the National Academy of Sciences of the United States of America, 2012, 109, 20455-20460.	3.3	162
18	Two structural configurations of the skeletal muscle calcium release channel. Nature Structural and Molecular Biology, 1996, 3, 547-552.	3.6	161

#	Article	IF	CITATIONS
19	Structural Analysis of Macromolecular Assemblies by Electron Microscopy. Chemical Reviews, 2011, 111, 7710-7748.	23.0	146
20	Structure of alpha-latrotoxin oligomers reveals that divalent cation-dependent tetramers form membrane pores. Nature Structural Biology, 2000, 7, 48-53.	9.7	128
21	The Escherichia coli large ribosomal subunit at 7.5 Ã resolution. Structure, 1999, 7, 1575-1583.	1.6	127
22	Three-dimensional structure of low density lipoproteins by electron cryomicroscopy. Proceedings of the National Academy of Sciences of the United States of America, 1999, 96, 8420-8425.	3.3	126
23	Structure of a viral DNA gatekeeper at 10 A resolution by cryo-electron microscopy. EMBO Journal, 2003, 22, 1255-1262.	3.5	124
24	Structure of bacteriophage SPP1 tail reveals trigger for DNA ejection. EMBO Journal, 2007, 26, 3720-3728.	3.5	120
25	Structure of Lumbricus terrestris Hemoglobin at 30 Ã Resolution Determined Using Angular Reconstitution. Journal of Structural Biology, 1995, 114, 28-40.	1.3	119
26	The structure of p53 tumour suppressor protein reveals the basis for its functional plasticity. EMBO Journal, 2006, 25, 5191-5200.	3.5	113
27	Structure of bacteriophage SPP1 head-to-tail connection reveals mechanism for viral DNA gating. Proceedings of the National Academy of Sciences of the United States of America, 2009, 106, 8507-8512.	3.3	107
28	Removal of Divalent Cations Induces Structural Transitions in Red Clover Necrotic Mosaic Virus , Revealing a Potential Mechanism for RNA Release. Journal of Virology, 2006, 80, 10395-10406.	1.5	106
29	Topologies of a Substrate Protein Bound to the Chaperonin GroEL. Molecular Cell, 2007, 26, 415-426.	4.5	96
30	Correlation functions revisited. Ultramicroscopy, 1992, 46, 307-316.	0.8	91
31	Dodecameric Structure of the Small Heat Shock Protein Acr1 from Mycobacterium tuberculosis. Journal of Biological Chemistry, 2005, 280, 33419-33425.	1.6	91
32	Structural organisation of the head-to-tail interface of a bacterial virus 1 1Edited by T. Richmond. Journal of Molecular Biology, 2001, 310, 1027-1037.	2.0	88
33	Multiple Distinct Assemblies Reveal Conformational Flexibility in the Small Heat Shock Protein Hsp26. Structure, 2006, 14, 1197-1204.	1.6	87
34	Structure of the VirB4 ATPase, alone and bound to the core complex of a type IV secretion system. Proceedings of the National Academy of Sciences of the United States of America, 2012, 109, 11348-11353.	3.3	86
35	Structure of a bacterial type IV secretion core complex at subnanometre resolution. EMBO Journal, 2013, 32, 1195-1204.	3.5	85
36	α-Latrotoxin, Acting via Two Ca2+-dependent Pathways, Triggers Exocytosis of Two Pools of Synaptic Vesicles. Journal of Biological Chemistry, 2001, 276, 44695-44703.	1.6	79

#	Article	IF	CITATIONS
37	Structure of a VirD4 coupling protein bound to a VirB type <scp>IV</scp> secretion machinery. EMBO Journal, 2017, 36, 3080-3095.	3.5	79
38	Detection and separation of heterogeneity in molecular complexes by statistical analysis of their two-dimensional projections. Journal of Structural Biology, 2008, 162, 108-120.	1.3	75
39	Globular Tetramers of β2-Microglobulin Assemble into Elaborate Amyloid Fibrils. Journal of Molecular Biology, 2009, 389, 48-57.	2.0	73
40	Localisation of the PsbH subunit in photosystem II: a new approach using labelling of his-tags with a Ni2+-NTA gold cluster and single particle analysis. Journal of Molecular Biology, 2001, 312, 371-379.	2.0	66
41	Structure of the 13-fold symmetric portal protein of bacteriophage SPP1. Nature Structural Biology, 1999, 6, 842-846.	9.7	62
42	Dynamic force microscopy imaging of native membranes. Ultramicroscopy, 2003, 97, 229-237.	0.8	62
43	Recognition and Separation of Single Particles with Size Variation by Statistical Analysis of their Images. Journal of Molecular Biology, 2004, 336, 453-460.	2.0	61
44	Elongated Oligomers Assemble into Mammalian PrP Amyloid Fibrils. Journal of Molecular Biology, 2006, 357, 975-985.	2.0	61
45	4.6à Cryo-EM reconstruction of tobacco mosaic virus from images recorded at 300keV on a 4k×4k CCD camera. Journal of Structural Biology, 2010, 171, 303-308.	1.3	61
46	Nanoscale stiffness topography reveals structure and mechanics of the transport barrier in intact nuclear pore complexes. Nature Nanotechnology, 2015, 10, 60-64.	15.6	57
47	Structural biology of the p53 tumour suppressor. Current Opinion in Structural Biology, 2009, 19, 197-202.	2.6	56
48	Cryo-EM structure of a type IV secretion system. Nature, 2022, 607, 191-196.	13.7	56
49	Structural rearrangements in the phage head-to-tail interface during assembly and infection. Proceedings of the National Academy of Sciences of the United States of America, 2015, 112, 7009-7014.	3.3	53
50	Use of chimeric type <scp>IV</scp> secretion systems to define contributions of outer membrane subassemblies for contactâ€dependent translocation. Molecular Microbiology, 2017, 105, 273-293.	1.2	49
51	Structure determination of macromolecular assemblies by single-particle analysis of cryo-electron micrographs. Current Opinion in Structural Biology, 2004, 14, 584-590.	2.6	48
52	Capsid Structure and Its Stability at the Late Stages of Bacteriophage SPP1 Assembly. Journal of Virology, 2012, 86, 6768-6777.	1.5	46
53	Quaternary structure of the specific p53–DNA complex reveals the mechanism of p53 mutant dominance. Nucleic Acids Research, 2011, 39, 8960-8971.	6.5	43
54	Tetramerisation of α-latrotoxin by divalent cations is responsible for toxin-induced non-vesicular release and contributes to the Ca2+-dependent vesicular exocytosis from synaptosomes. Biochimie, 2000, 82, 453-468.	1.3	41

#	Article	lF	CITATIONS
55	Mutant α-Latrotoxin (LTXN4C) Does Not Form Pores and Causes Secretion by Receptor Stimulation. Journal of Biological Chemistry, 2003, 278, 31058-31066.	1.6	40
56	Quaternary structure of the liver microsomal cytochrome P-450. FEBS Letters, 1986, 205, 35-40.	1.3	39
57	Voltage-gated K+ Channel from Mammalian Brain: 3D Structure at 18à of the Complete (α)4(β)4 Complex. Journal of Molecular Biology, 2003, 326, 1005-1012.	2.0	39
58	Genome Gating in Tailed Bacteriophage Capsids. Advances in Experimental Medicine and Biology, 2012, 726, 585-600.	0.8	39
59	Methods for Three-Dimensional Reconstruction of Heterogeneous Assemblies. Methods in Enzymology, 2010, 482, 321-341.	0.4	38
60	Escherichia coli RNA polymerase core and holoenzyme structures. EMBO Journal, 2000, 19, 6833-6844.	3.5	35
61	Hexameric ring structure of human MCM10 DNA replication factor. EMBO Reports, 2007, 8, 925-930.	2.0	35
62	Molecular structure of human geminin. Nature Structural and Molecular Biology, 2004, 11, 1021-1022.	3.6	34
63	Lengsin Is a Survivor of an Ancient Family of Class I Glutamine Synthetases Re-engineered by Evolution for a Role in the Vertebrate Lens. Structure, 2006, 14, 1823-1834.	1.6	33
64	Structures of biomolecular complexes by combination of NMR and cryoEM methods. Current Opinion in Structural Biology, 2017, 43, 104-113.	2.6	32
65	The ribosome and its role in protein folding: looking through a magnifying glass. Acta Crystallographica Section D: Structural Biology, 2017, 73, 509-521.	1.1	32
66	Structural Analysis of the Saf Pilus by Electron Microscopy and Image Processing. Journal of Molecular Biology, 2008, 379, 174-187.	2.0	31
67	Electron microscopy of beef heart mitochondrial F1 -ATPase. FEBS Letters, 1984, 167, 285-290.	1.3	30
68	Structure of Triglyceride-Rich Human Low-Density Lipoproteins According to Cryoelectron Microscopy. Biochemistry, 2003, 42, 14988-14993.	1.2	30
69	Novel Inter-Subunit Contacts in Barley Stripe Mosaic Virus Revealed by Cryo-Electron Microscopy. Structure, 2015, 23, 1815-1826.	1.6	28
70	Two p53 tetramers bind one consensus DNA response element. Nucleic Acids Research, 2016, 44, 6185-6199.	6.5	28
71	An Expanded and Flexible Form of the Vacuolar ATPase Membrane Sector. Structure, 2006, 14, 1149-1156.	1.6	26
72	The structural basis for Z α ₁ -antitrypsin polymerization in the liver. Science Advances, 2020, 6, .	4.7	26

#	Article	IF	CITATIONS
73	Structural organisation of the type IV secretion systems. Current Opinion in Microbiology, 2014, 17, 24-31.	2.3	25
74	Quaternary Structure of the European Spiny Lobster (Palinurus elephas) 1×6-mer Hemocyanin from cryoEM and Amino Acid Sequence Data. Journal of Molecular Biology, 2003, 325, 99-109.	2.0	24
75	Bacteriophage SPP1 Tail Tube Protein Self-assembles into β-Structure-rich Tubes. Journal of Biological Chemistry, 2015, 290, 3836-3849.	1.6	24
76	Structure of the ATP-synthase studied by electron microscopy and image processing. FEBS Letters, 1989, 244, 279-282.	1.3	23
77	Structural transitions during the scaffolding-driven assembly of a viral capsid. Nature Communications, 2019, 10, 4840.	5.8	21
78	The SPP1 connection. FEMS Microbiology Reviews, 1995, 17, 47-56.	3.9	20
79	Three-Dimensional Structure of Keyhole Limpet Hemocyanin by Cryoelectron Microscopy and Angular Reconstitution. Journal of Structural Biology, 1995, 115, 226-232.	1.3	20
80	Intrinsic versus imposed curvature in cyclical oligomers: the portal protein of bacteriophage SPP1 EMBO Journal, 1996, 15, 4785-4788.	3.5	20
81	Structure of the hDmc1-ssDNA Filament Reveals the Principles of Its Architecture. PLoS ONE, 2010, 5, e8586.	1.1	20
82	On the negative staining of the protein crystal structure. Ultramicroscopy, 1981, 7, 131-137.	0.8	17
83	Structural Study of Heterogeneous Biological Samples by Cryoelectron Microscopy and Image Processing. BioMed Research International, 2017, 2017, 1-23.	0.9	17
84	Structural Analysis of Protein Complexes by Cryo Electron Microscopy. Methods in Molecular Biology, 2017, 1615, 377-413.	0.4	15
85	Structural analysis of non-crystalline macromolecules: the ribosome. Acta Crystallographica Section D: Biological Crystallography, 2000, 56, 1253-1258.	2.5	11
86	Computer averaging of 50 S ribosomal subunit electron micrographs. Journal of Molecular Biology, 1983, 169, 345-350.	2.0	10
87	Electron microscopy of the Mo-Fe-protein from Azotobacter vinelandii nitrogenase. FEBS Journal, 1985, 149, 389-392.	0.2	10
88	How viruses infect bacteria?. EMBO Journal, 2009, 28, 797-798.	3.5	10
89	Strand-like structures and their three-dimensional organization in the large subunit of theEscherichia coli ribosome. Molecular Biology Reports, 1982, 8, 191-197.	1.0	9
90	Electron microscopy of multiple forms of glutamine synthetase from bacteroids and the cytosol of yellow lupin root nodules. BBA - Proteins and Proteomics, 1987, 913, 368-376.	2.1	9

#	Article	IF	CITATIONS
91	HREM of epitaxial layers in the InAs/GaAs system. Ultramicroscopy, 1991, 35, 11-18.	0.8	9
92	Structural basis for DNA strand separation by a hexameric replicative helicase. Nucleic Acids Research, 2015, 43, 8551-8563.	6.5	9
93	DNA Induces Conformational Changes in a Recombinant Human Minichromosome Maintenance Complex. Journal of Biological Chemistry, 2015, 290, 7973-7979.	1.6	8
94	Unwinding of a DNA replication fork by a hexameric viral helicase. Nature Communications, 2021, 12, 5535.	5.8	8
95	On the fine structure of rat liver ribosome small subunits. Molecular Biology Reports, 1982, 8, 185-189.	1.0	6
96	Bacteriophages: Their Structural Organisation and Function. , 0, , .		6
97	Unravelling Ribosome Function Through Structural Studies. Sub-Cellular Biochemistry, 2019, 93, 53-81.	1.0	6
98	Determination of Escherichia coli RNA Polymerase Structure by Single Particle Cryoelectron Microscopy. Methods in Enzymology, 2003, 370, 24-42.	0.4	4
99	Fine structure of the 30 S ribosomal subunit. FEBS Letters, 1985, 186, 21-25.	1.3	2
100	Electron microscopy of the nitrogenase molecule from azotobacter vinelandii. Journal of Inorganic Biochemistry, 1986, 27, 141-146.	1.5	2
101	A molecular syringe that kills cells. Nature Structural and Molecular Biology, 2015, 22, 357-359.	3.6	2
102	The absence or presence of a lytic coliphage affects the response of Escherichia coli to heat, chlorine, or UV exposure. Folia Microbiologica, 2018, 63, 599-606.	1.1	2
103	The Skeletal Muscle Calcium-Release Channel Visualised By Electron Cryomicroscopy and Angular Reconstitution. , 1998, , 23-46.		2
104	Intrinsic versus imposed curvature in cyclical oligomers: the portal protein of bacteriophage SPP1. EMBO Journal, 1996, 15, 4785-8.	3.5	2
105	The SPP1 connection. , 0, .		1
106	Visualization of the Translational Elongation Cycle by Cryo-Electron Microscopy. , 0, , 35-44.		1
107	Structural studies of T4S systems by electron microscopy. AIMS Biophysics, 2015, 2, 184-199.	0.3	1
108	Cryo-EM Structures of Two Bacteriophage Portal Proteins Provide Insights for Antimicrobial Phage Engineering. Viruses, 2021, 13, 2532.	1.5	1

#	Article	IF	CITATIONS
109	The Structure of Red Clover Necrostic Mosaic Dianthovirus at 10 Ã Resolution. Microscopy and Microanalysis, 2004, 10, 1486-1487.	0.2	0
110	Lysis Performance of Bacteriophages with Different Plaque Sizes and Comparison of Lysis Kinetics After Simultaneous and Sequential Phage Addition. Phage, 2020, 1, 149-157.	0.8	0
111	Correlation Averaging and Filtering of Electron Micrographs. , 1991, , 327-332.		0
112	3-D structure of single macromolecules at 15Ã resolution by cryo-microscopy and angular reconstitution. Proceedings Annual Meeting Electron Microscopy Society of America, 1995, 53, 838-839.	0.0	0